

Estimation of Mode-III Interlaminar Fracture Toughness in GFRP Laminates



J.V. Sai Prasanna Kumar

Abstract: The composite material is heterogenous in nature has several applications ranging from sports to defence industries replacing the conventional materials. Assessing the strength composite material for out of plane delamination characterization is a challenging task. One of the test specimens which can simulate the out of the plane loading is the Edge crack torsion (ECT) specimen, to study the delamination growth in composite laminates in a controlled environment. For the present work a fixture was developed to simulate out of plane loading and hence to estimate mode-III fracture toughness. The test coupons were cast using from bi-directional satin glass fibre woven mat, subsequently a starter crack was introduced in the mid plane. A 100 KN Instron Universal test loading frame was used in static condition. It was observed that the crack growth did initiate from specimen centre. The fracture parameter experimentally measured was found to be dependent on the crack growth.

Keywords: Delamination, Edge Crack Torsion Test Specimen Fracture toughness, GFRP Mode III, Out of Plane Loading, Radiographic Scanning

I. INTRODUCTION

New class of polymer composite materials gained entry in aircraft industry in 1960's and the response of these materials under harsh conditions requires a deep knowledge of the behaviour materials. The attractive characteristics of composite materials are its high strength, light weight, and fatigue resistance.

Both closed form and numerical solutions are available to obtain the fracture parameters of polymer composites. The opening and shear mode studies were undertaken by several researchers, employing data reduction schemes and validating the results numerically. Even Mixed mode characterization was attempted by several researchers. But out of plane characterizations in polymer composites was attempted only by a very few researchers, because mode- I & mode- II delamination play a dominant role in propagating the damage in the material. But in all these studies a fracture-based approach is used.

Quasi static tests are enough to determine the fracture parameters without stress raisers, and if there are defects either macroscopic or microscopic are present and these flaws will become dominant leading to catastrophic failure. The harsh environment is significant at the crack tip and contribute to delamination growth.

In metals, local deformation due to high loads, reduces stress intensity factor [1-4]. These high stresses will cause crack to propagate along the specimen. Both type of fracture would eventually fail due to excessive loading and thus defining fracture toughness as the amount of energy necessary to create the fracture surface.

At room temperatures considerable energy is required for fracture to occur with parameters such as applied loads, existing defects, rates of propagation of the defects will significantly affect the structural integrity of the material. Generally, the material behaviour is elastic in regions far away from crack. But at crack tip the fracture toughness is determined by energy release rate G [5-6].

Defects are predominant in polymer composites either intentional or unintentional, often in polymer composites it is the combination of both brittle ductile behaviour such as matrix cracking, inter laminar fracture, debonding, fibre pull-out. Interlaminar fracture is the major problem associated with polymer composites leading to failure of the material [7-9]. The parameter G representing growth of the flaw under different loading conditions [10-11]]. ASTM standards are available for delamination tests in opening and shear mode [12-13], while for the out of plane loading standards are underway.

II. FIXTURE DESIGN

In this present work a fixture was designed to simulate the pure out of plane loading on the glass fibre reinforced plastics. The fixture designed was used for pure mode-III testing. It has columns, located opposite to each other, and they contain vertical holes to be attached to UTM'S jack, Fig 1. The load is applied through the provisions mounted on the blocks and they are attached to the loading frame of Instron test machine.



Figure 1 Modified Fixture

Revised Manuscript Received on December 30, 2019.

* Correspondence Author

J.V. Sai Prasanna Kumar, Department of Aeronautical Engineering
Vel Tech Rangarajan Dr Sagunthala R&D Institute of Science and
Technology Chennai-600052. Email: saiprasannajv1202@gmail.com

© The Authors. Published by Blue Eyes Intelligence Engineering and Sciences Publication (BEIESP). This is an open access article under the CC BY-NC-ND license (<http://creativecommons.org/licenses/by-nc-nd/4.0/>)

The fixture is fabricated using two aluminium blocks supplied by Hind Aluminium; Chennai with dimensions of 150 mm x 85 mm x 35 mm, with Supports at 76 mm apart. Provisions were also made on the fixture to be mounted into the Instron loading frame. The line sketch of the coupon shown in figure 2, having following dimensions. The total length of the specimen is 108 mm distance between the loading pins $w = 32$ mm, $l = 72$ mm, $b = 38$ mm, the thickness of the specimen is 6 mm. Coupons with various starter cracks lengths were fabricated.

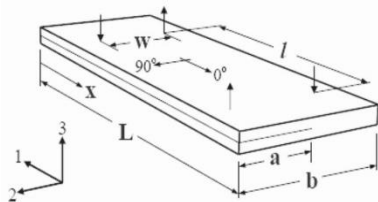


Figure 2 Specimen geometry

III. MATERIALS AND METHODS

3.1 Sample fabrication

A satin woven bi-directional glass matt was purchased from M/S St. Gobain, the polymer resins LY566 was obtained from M/S Huntsman Ltd, Chennai, TETA an aromatic compound was used as the hardening agent. A laminate of size 300 mm x 300 mm was fabricated using wet lay-up technique and was left over night for curing at room temperature. Post curing was done according to manufacturer’s specification. The samples were machined to the desired dimensions. Generally precracking is to be introduced in the samples either by using jeweller’s saw or by a thin film. The second method was adopted for this work the material properties are listed in table 1.

Table 1 Material Properties

SL.NO	Property	Value
1	E11	47.71GPa
2	E22	12.27GPa
3	E33	12.27GPa
4	G12	4.83GPa
5	G13	4.83GPa
6	G23	4.48GPa
7	v12	0.278
8	v13	0.278
9	v23	0.403

3.2 Testing

The test fixture is mounted on quasi static 100 KN Instron universal testing machine. Specimens were mounted on the test fixture, taking care to align the specimen along the load frame. After levelling the specimens were tested in displacement-controlled environment along with rate of

the crosshead movement till failure fig 3 & fig 4. The displacement curves were machine generated, and maximum load was noted.



Figure 3 Specimen in UTM



Figure 4

Testing in progress

3.3. Data reduction Scheme

There are several reduction schemes available to calculate initiation values of G_{IIIc} . The description of the data reduction schemes is found elsewhere [12]. The compliance of each specimen, (C), can be obtained from the load vs displacement plot.

The stiffness (1/C), was expressed as,
 $1/C = [1-(a/b)]$ (1)

Where $C = \delta / P$, δ is the displacement of the specimen in mm. P is the load. The constants A, m can be obtained by linear regression. The fracture parameter of each test coupon was calculated based on the maximum load, P_c^{max} , and with onset of nonlinearity, P_c^{NL}
 $G_{II}(max) = mC (P_c^{max})^2 / 2lb[1-m(a/b)]$ (2)

$G_{II}(NL) = mC (P_c^{NL})^2 / 2lb[1-m(a/b)]$ (3)
 $G_{II}(max)$ and $G_{IIIc}(NL)$, were then plotted. The critical strain energy release rate values vary as flaw initiation.

IV. EXPERIMENTAL RESULTS

The load-displacement response of the test coupon is presented in Figure 5. There is a nonlinear response phase followed by the linear region with a sudden load drop in the curve is observed. Table 2, 3 and 4 shows experimentally measured constants for different a/b ratios.

Table 2 Load displacement values for different a/b = 0.2

Sample 1		sample 2		sample 3	
load(N)	Displacement (mm)	load(N)	Displacement (mm)	load(N)	Displacement (mm)
0	0	0	0	0	0
250	1.5	200	1.2	200	0.7
500	2.75	400	1.6	400	1.6
750	4	600	2.3	600	2.7
1000	4.95	800	2.9	800	4.3
1250	6.5	1000	3.8	1000	6
1500	9	1200	4.7	1200	9.1
1703	15.26	1400	6.4	1400	10.3
		1600	9.6	1542	12.45
		1654	13.46		

Table 3 Load displacement values for a/b = 0.4

Sample 1		Sample 2		Sample 3	
load(N)	Displacement (mm)	load(N)	Displacement (mm)	load(N)	Displacement (mm)
0	0	0	0	0	0
200	0.75	250	1.6	200	1.4
400	1.7	500	2.5	400	2.2

600	2.5	750	4	600	3.4
800	3.4	1000	5.4	800	4.5
1000	4.6	1250	7	1000	5.5
1200	6.2	1500	8.9	1200	6.8
1400	8.1	1717	12.14	1298	9.81
1563	11.8	1689	12.9		

Table 4 Load displacement values for a/b =0.6

Sample 1		Sample 2		Sample 3	
load(N)	Displacement (mm)	load(N)	Displacement (mm)	load(N)	Displacement (mm)
0	0	0	0	0	0
200	1.3	200	1.5	200	1.4
400	3	400	2.1	400	2.9
600	4.2	600	3	600	4.1
800	6	800	3.8	800	6.3
1000	8.3	1000	4.5	1000	7.4
1200	11.94	1200	6.7	1175	11.49
1290	14.74	1360	13.34		

V. RESULT AND DISCUSSION

Along the delamination front, G_{III} , was inversely proportional to the increase on insert length. The figures 5-7 shows the load vs displacement pattern for various a/b ratios. The trend in figure 8 has distribution which was asymmetrical.[7]. The load and supports would create a sliding movement parallel to direction of delamination growth. The pressure at the supports was minimum except at the supports. The G_I contribution to G_{III} could be negligible.

The sliding friction generated by the movement of the delamination front surfaces was not considered because of its insignificant effect, table 6.

The results indicate that the out of plane dominated delamination growth takes place from the centre. Samples were examined using radiographic technique at the crack front matrix cracking along the front can be observed fig 9-10.

Table 6 Strain Energy Release Rate

a/b	G _{IIIc} (max)	G _{IIIc} (NL)
	(N/mm)	(N/mm)
0.3	6.08	4.674
0.4	11.371	9.371
0.5	15.18	11.819

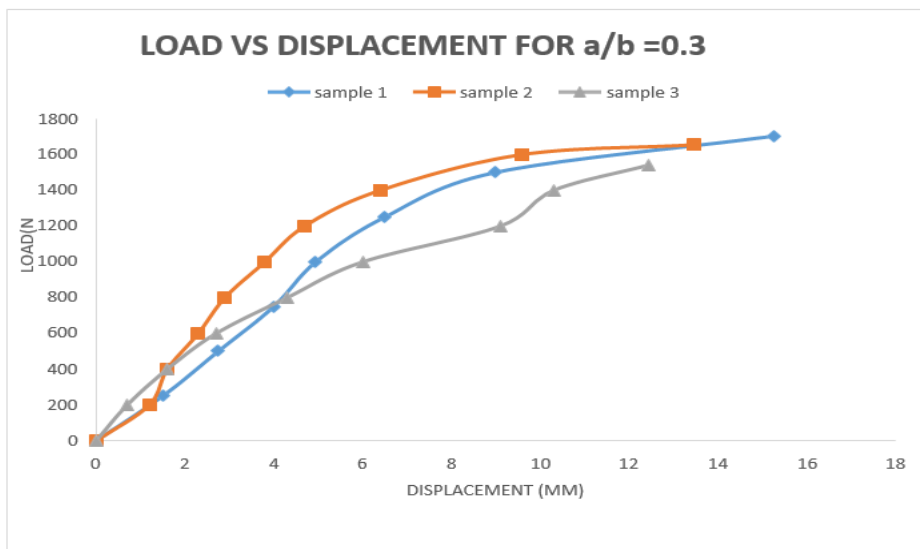


Figure 5 Load VS Displacement for a/b=0.3

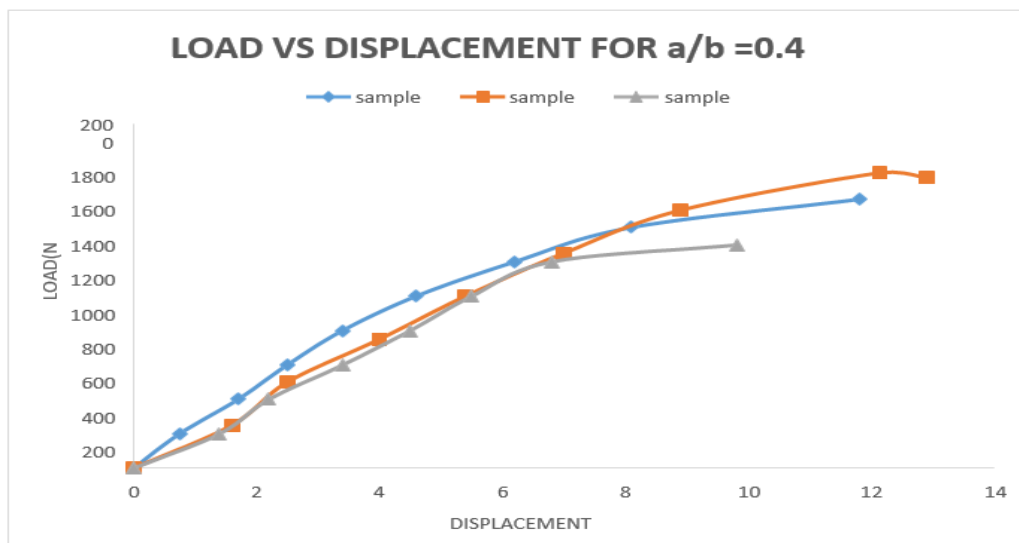


Figure 6 Load VS Displacement for a/b=0.4

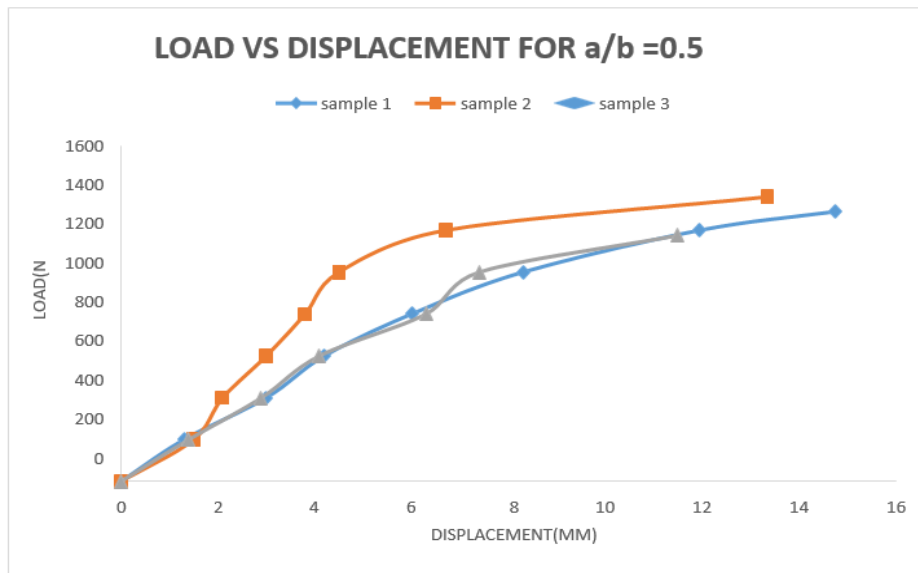


Figure 7 Load VS Displacement for a/b=0.3

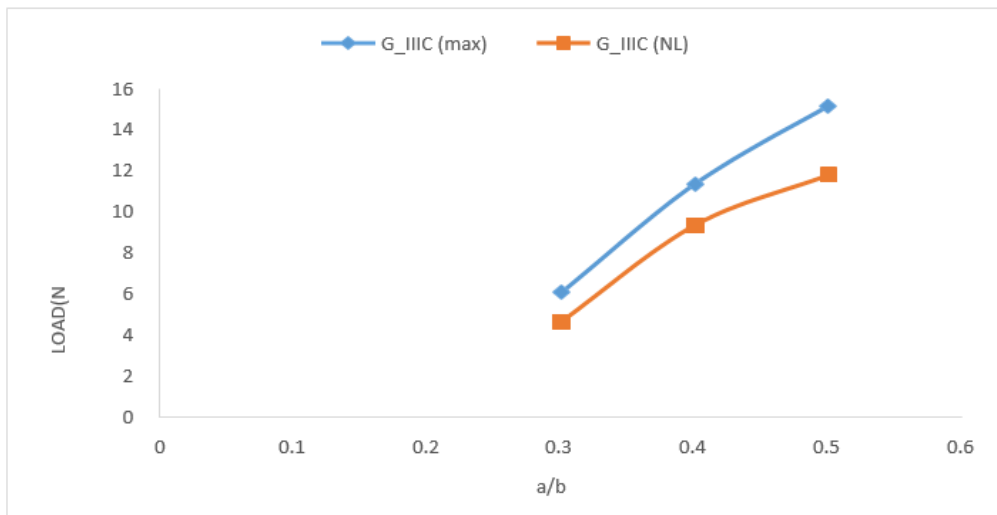


Figure 8 Critical Strain Energy Release Rate vs, a/b

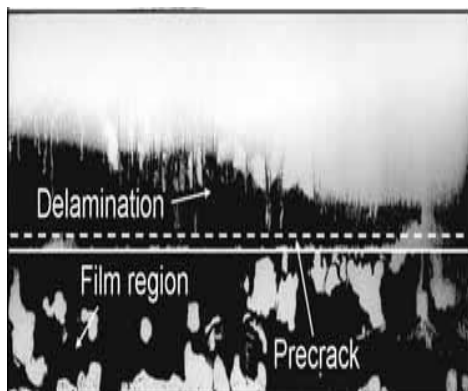


Figure 9 Simple Examined at the Delamination Front

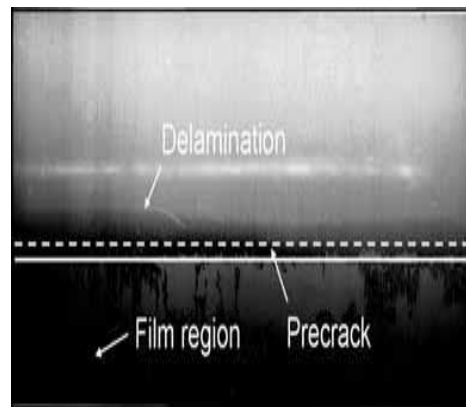


Figure 10 Simple Examined at Crack Front

Determination of out of plane fracture toughness the maximum load may not be realistic due to the presence of starter crack,

VI. CONCLUSION

With the completion of coupon level tests conducted at ambient conditions, these points may be mentioned

1. Fracture mechanics-based approach namely compliance calibrations method was utilized for out of plane characterization depending on the deterioration of the material stiffness
2. The fixture thus developed could be utilized for simulating anti-plane crack characterization for any composite material system.
3. It can be observed that G_{IIIc} increases with the crack length increases.
4. In this experimental study a new two-point loading fixture was designed, and it can simulate the anti-plane delamination growth.
7. Acknowledgement The author wishes to thank the management for providing the facilities to conduct the research work and the Mr. Ashok Kumar deserves a special mention in testing the samples at short notices. Radiographic was carried out at NDT services in Chennai
8. Conflict of Interest

There was no conflict of interest in preparing this document

VII. REFERENCES

1. Ratcliffe, J. G. "Characterization of the Edge Crack Torsion (ECT) Test for Mode III Fracture Toughness Measurement of Laminated Composites, NASA/TM-2004-213269, 2004.
2. Lee, S. M. "An Edge Crack Torsion Method for Mode III Delamination Fracture Testing," Journal of Composites Technology & Research, JCTRER, Vol.15, No.3, 1993, pp.193-201
3. Li, J., Lee, S. M., Lee, E. W., and O'Brien, T. "Evaluation of the Edge Crack Torsion (ECT) Test for Mode III Interlaminar.
4. Fracture Toughness of Laminated Composites," Journal of Composites Technology & Research, JCTRER, Vol.19, No.3, 1997, pp.174-183.
5. Suemasu, H. "An Experimental Method to Measure the Mode-III Interlaminar Fracture Toughness of Composite Laminates," Composites Science and Technology, 1999, pp.1015-1021
6. F. Sharif, M.T. Kortschot, R.H. Martin, Mode III delamination using a split cantilever beam, in: R.H. Martin (Ed.), Composite Materials: Fatigue and Fracture vol.5, ASTM STP 1230, ASTM, Philadelphia, 1995, pp.85-99.
7. B.D. Davidson, F.O. Sediles, Mixed-mode I-II-III delamination toughness determination via a shear torsion bending test, Compos Part A 42 (2011), pp.589-603.
8. J.Li, T.K. Ó'Brien, Simplified data reduction methods for the ECT test for mode III interlaminar fracture toughness, J. Compos Technol. Res. 18 (1996), pp. 96-101
9. A.B. de Moraes, A.B. Pereira, Mixed mode II and III interlaminar fracture of carbon/epoxy laminates, Compos Sci. Technol. 68 (2008), pp.2022-2027.
10. F.A. Mehrabadi, Analysis of pure mode III and mixed mode (III & II) inter-laminar crack growth in polymeric woven fabrics, Mater Des. 44 (2013), pp. 429-437.
11. E.F. Rybicki, M.F. Kanninen, A finite element calculation of stress intensity factors by a modified crack closure integral, Eng. Fract. Mech. 9 (1977), pp. 931-938.
12. H. Tada, P.C. Paris, G.R. Irwin, The stress analysis of cracks handbook, 1973.
13. J.Li, T.K. Ó'Brien, Simplified data reduction methods for the ECT test for mode III interlaminar fracture toughness, J. Compos Technol. Res. 18 (1996), pp. 96-101.

AUTHORS PROFILE



J. V. SaiPrasanna Kumar, graduated, from IIT(M) in Aerospace Engineering. Obtained Ph.D. from Anna University in Composite materials. NDT, Fracture Mechanics and Composite materials are his areas of interest.